Hindawi Publishing Corporation
Journal of Nanomaterials
Volume 2013, Article ID 434197, 7 pages
http://dx.doi.org/10.1155/2013/434197

Research Article

Synthesis and Characterization of $CeVO_4$ by Microwave Radiation Method and Its Photocatalytic Activity

Nuengruethai Ekthammathat,[1] Titipun Thongtem,[1] Anukorn Phuruangrat,[2] and Somchai Thongtem[3,4]

[1] *Department of Chemistry, Faculty of Science, Chiang Mai University, Chiang Mai 50200, Thailand*
[2] *Department of Materials Science and Technology, Faculty of Science, Prince of Songkla University, Hat Yai, Songkhla 90112, Thailand*
[3] *Department of Physics and Materials Science, Faculty of Science, Chiang Mai University, Chiang Mai 50200, Thailand*
[4] *Materials Science Research Center, Faculty of Science, Chiang Mai University, Chiang Mai 50200, Thailand*

Correspondence should be addressed to Titipun Thongtem; ttpthongtem@yahoo.com
and Anukorn Phuruangrat; phuruangrat@hotmail.com

Received 1 June 2013; Revised 7 August 2013; Accepted 8 August 2013

Academic Editor: Jiaguo Yu

Copyright © 2013 Nuengruethai Ekthammathat et al. This is an open access article distributed under the Creative Commons Attribution License, which permits unrestricted use, distribution, and reproduction in any medium, provided the original work is properly cited.

A general microwave synthesis method was developed to synthesize cerium orthovanadate ($CeVO_4$) nanostructures without the use of any catalysts or templates. This method is able to control the shape and size of the products by adjusting the pH of precursor solutions to be 1–10. Phase, purity, and different morphologies of the products were characterized by XRD, FTIR, SEM, and TEM. They showed that the as-synthesized products exhibited pure single crystalline $CeVO_4$ with tetragonal structure. Their morphologies developed in sequence as nanoparticles (pH = 4–10), nanorods (pH = 2, 3), and microflowers (pH = 1). UV-visible spectra were used to estimate the direct energy gaps of $CeVO_4$ nanorods and microflowers: 3.77 and 3.65 eV, respectively. Photoluminescence (PL) of $CeVO_4$ microflowers showed strong emission intensities at 578 nm. These results were in the range of possible application for photocatalysis, investigated by studying the degradation of methylene blue.

1. Introduction

In recent years, nanostructured rare earth orthovanadates (RVO_4), an important compound family of inorganic materials, have been widely studied due to their important properties [1, 2]. Generally, the RVO_4 structure has two polymorphs: a monoclinic monazite type and a tetragonal zircon type [2]. Phase of the individual RVO_4 was influenced by the ionic radii of rare earth elements. Due to the higher coordination number, the larger rare earth elements prefer to crystallize in the monazite type, as compared to the zircon one [2]. For $CeVO_4$, it is in between the boundary of the first and second types, controlled by the synthesis conditions [2]. Cerium orthovanadate ($CeVO_4$) is an interesting phase of the Ce-V-O ternary system and has a tetragonal zircon-type structure belonging to the space group I41/amd [3–6]. This tetragonal zircon-type structure stabilizes Ce^{3+} cations even in an oxidizing condition [3]. The compound exhibits unique electronic [6–8], optical [6–10], magnetic [6–10], catalytic [9, 10], and luminescent [9, 10] properties. It has wide potential application in various fields, such as oxidative catalyst [7, 10, 11, 13], gas sensors [7, 11, 12], luminescence [7, 10], electrochromic material [9, 13], and components of solid oxide fuel cells (SOFCs) [11–13].

Photocatalysis by solar energy is of great importance in solving global energy and environmental crises [14, 15]. They have been applied in many fields like waste water treatment, air purification, water splitting to produce hydrogen gas, and other environmental problems [9, 15, 16]. It was also reported that lanthanide orthovanadates can be used as photocatalysts for the degradation of dyes and organic compounds [17]. Thus the particular 4f-5d and 4f-4f electronic transitions are different from other elements [7]. The photocatalytic activities of rare earth orthovanadates for the degradation of methylene blue were also reported by Mahapatra et al. [4] and Selvan et al. [2].

Most previous approaches for the synthesis of cerium orthovanadate were reported: hydrothermal method [1, 7, 13],

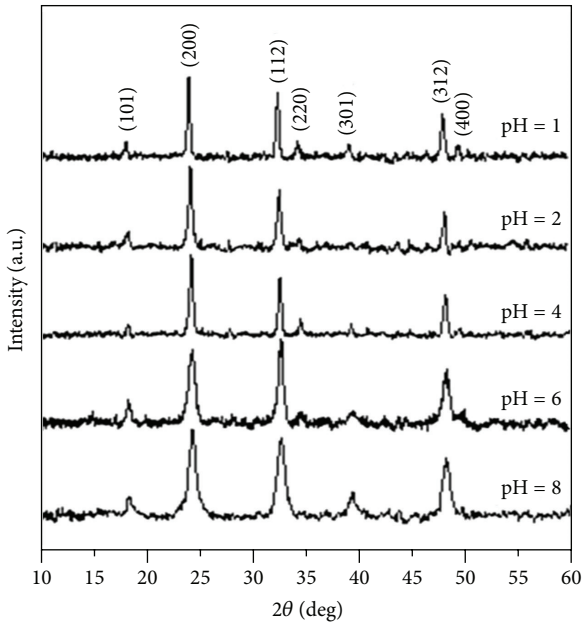

Figure 1: XRD patterns of $CeVO_4$ synthesized in the solutions with the pH of 1, 2, 4, 6, and 8 by microwave radiation at 180 W for 120 min.

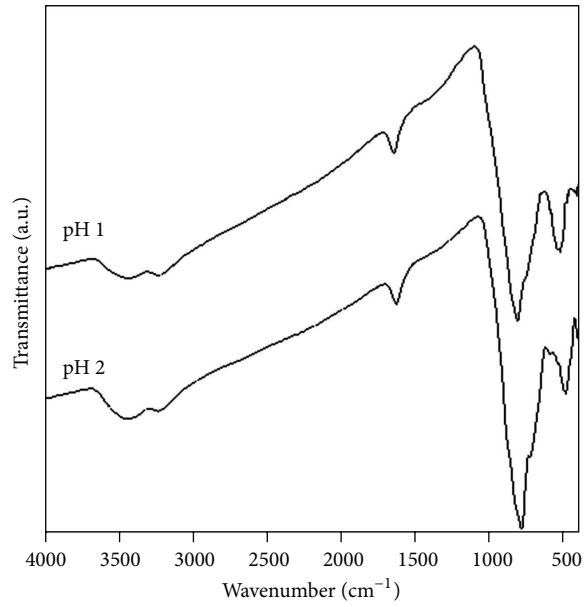

Figure 2: FTIR spectra of $CeVO_4$ synthesized in the solutions with the pH of 1 and 2 by microwave radiation at 180 W for 120 min.

sol-gel [5], sonochemical method [2, 10], and microwave-assisted synthesis [9, 11]. Microwave-assisted synthesis is an interesting process and is a rapidly developing area of the research. Microwave has been in use to accelerate organic reaction rate since it is generally fast, simple, and consume less energy. The energy transfer from microwave to the material is believed to be by resonance and relaxation, resulting in rapid heating [9, 11]. Moreover, microwave-assisted synthesis is unique in their potential for large-scale synthesis without suffering thermal gradient effect [18]. In this work, a simple microwave irradiation route was used to synthesize $CeVO_4$ nanorods and microflowers. The dependence of optical properties and photocatalytic application of $CeVO_4$ with different morphologies is reported.

2. Experimental Procedures

In a typical procedure, 0.005 mol $Ce(NO_3)_3{\cdot}6H_2O$ (cerium (III) nitrate hexahydrate, assay 99.50%, Acros) and 0.005 mol NH_4VO_3 (ammonium metavanadate, assay 100.3%, Baker analyzed A.C.S. Reagent) were dissolved in 80 mL DI water in a volumetric flask. The pH of the precursor solutions was adjusted to be 1–4 using HCl (assay 35.4%, BDH) and 5–10 using 3 M NaOH (assay 90.0%, Solvay) under vigorous stirring. The mixed solutions were stirred for 15 min and they turned into transparency solutions at the pH 1-2, red-brown precipitate at the pH 3-4, and yellow precipitate at the pH 5–10. The ready-adjusted mixture was then placed in a home type microwave oven (Electrolux, EMS 2820, 2.45 GHz) at 180 W and processed for 120 min to form precipitates. The as-synthesized precipitates were filtered, rinsed with DI water and 95% ethanol several times, and dried at 70°C for 24 h.

Crystalline degree and phase identification were analyzed by X-ray diffractometer (XRD, Philips X'Pert MPD) using a Cu-K_α radiation at 45 kV and 35 mA in the range of 10–60 deg. Size and morphology of the as-synthesized $CeVO_4$ were characterized by field emission scanning electron microscope (FE-SEM, JEOL JSM-6335F) operating at 35 kV. A transmission electron microscopic image and selected area electron diffraction (SAED) patterns of the as-synthesized $CeVO_4$ products were taken using a transmission electron microscope (TEM, JEOL JEM-2100F) operating at 200 kV. Fourier transform infrared (FTIR) spectrometer was carried out by a Perkin Elmer RX Spectrometer in the range of 400–4000 cm^{-1} at room temperature, with $CeVO_4$ tablets diluted 40-fold with KBr. The photoluminescence (PL) emission was studied by a LS 50B PerkinElmer fluorescence spectrophotometer using 420 nm excitation wavelength at room temperature. Absorbance spectra of a UV-visible spectrometer (Lambda 25 PerkinElmer) were used to analyze energy gap of the products and to determine the degradation of methylene blue at room temperature.

Photocatalysis was proceeding in a photoreactor fitted with three 15 W of UV germicidal irradiation lamps. The lamp irradiated predominantly at 365 nm (3.4 eV) and a photon flux of 5.8×10^{-6} mol/s [4, 9]. The photocatalytic activities were evaluated by measuring the photocatalytic degradation of methylene blue (MB) in the aqueous solutions. In a typical degradation experiment, 100 mL of 10^{-5} M MB solution and 100 mg as-synthesized cerium orthovanadate were put in a 250 mL Pyrex Erlenmeyer flask and the mixture was continuously stirred in the dark for 30 min to attain adsorption-desorption equilibrium of MB on surface of the photocatalyst. The equilibrium concentration of MB was used as the initial value for the photodegradation process. The light was turned on to initiate the photocatalytic reaction. At certain time intervals, every 5 mL solution was sampled and centrifuged to remove particles inside. The degradation of organic dye was monitored by measuring the absorbance of

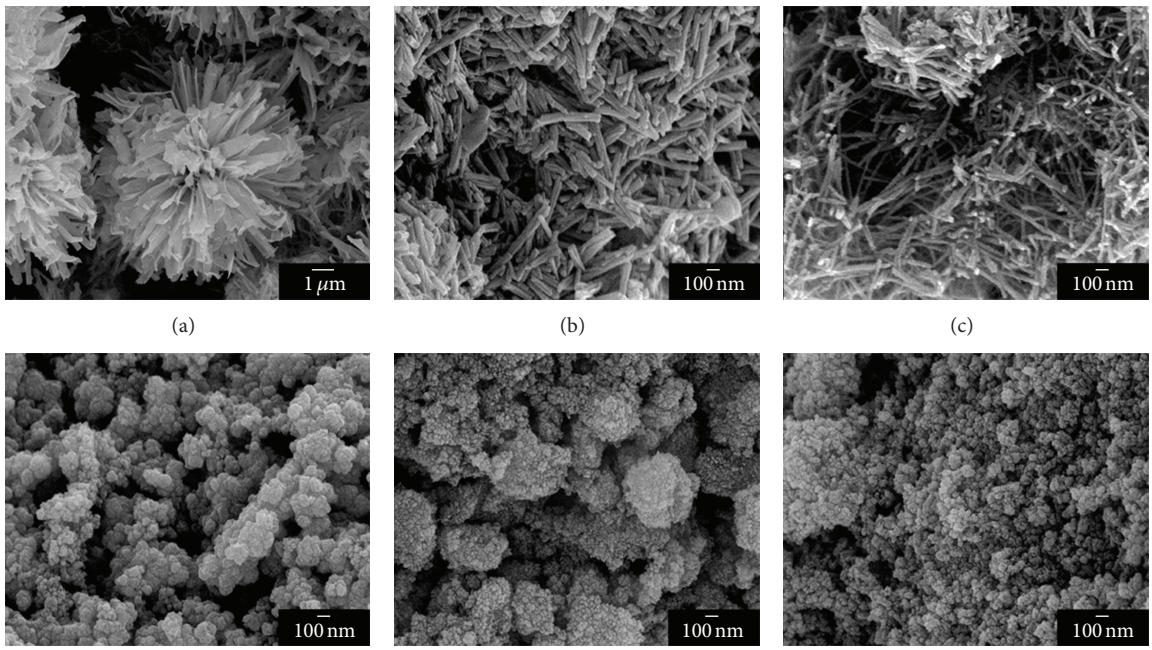

FIGURE 3: SEM images of $CeVO_4$ synthesized in the solutions with the pH of ((a)–(f)) 1, 2, 3, 4, 5, and 6 by microwave radiation at 180 W for 120 min.

the solutions with DI water as a reference and the degradation efficiency was determined from the absorbance intensity at 665 nm wavelength.

3. Results and Discussion

Phase, purity, and crystallinity of the as-synthesized cerium orthovanadate were characterized by powder X-ray diffraction. Figure 1 shows the XRD patterns of $CeVO_4$ synthesized in the solutions with the pH of 1, 2, 4, 6, and 8 by a microwave irradiation method at 180 W for 120 min. The patterns fitted well with the tetragonal (zircon) type $CeVO_4$ with I41/amd space group, lattice constants $a = b = 7.340$ Å and $c = 6.470$ Å of the JCPDS no. 72-0282 [19]. The diffraction peaks were carefully indexed and assigned to the lattice planes of (101), (200), (112), (220), (301), (312), and (400), corresponding to the 2θ values of 18.3, 24.2, 32.6, 34.5, 39.3, 48.2, and 49.6 deg., respectively. No other impurities were detected in these spectra. Upon increasing the acidity content of the precursor solutions, all the peaks became sharpened. Thus, they were concluded that the pH of the solutions plays an important role in the crystalline degree of pure $CeVO_4$ [3, 10, 11, 13, 17].

Figure 2 presents the FTIR spectra of $CeVO_4$ synthesized in the solutions with the pH of 1 and 2 by microwave radiation at 180 W for 120 min. The FTIR spectra were recorded over the range of 400–4,000 cm^{-1}. In this research, both spectra show sharp and broad bands around 460 cm^{-1} and 786 cm^{-1} due to the stretching vibration of VO_4 and V–O, respectively [2, 4, 5, 20, 21]. Other shallow bands of the O–H bending [2] and stretching [4, 20, 22] of water adsorbed on the surface of $CeVO_4$ were also detected at 1,620 and 3,420 cm^{-1}, respectively.

General morphologies and sizes of $CeVO_4$ were examined by FE-SEM technique. The FE-SEM images of the products (Figure 3) synthesized in the solutions with the pH of 1, 2, 3, 4, 5, and 6 showed different morphologies. The products exhibited microflowers at the pH 1 with diameters of about 10 μm, nanorods at the pH 2 and 3. For the pH 2, the product was nanorods about 600 nm long and about 50 nm in diameter. For the pH 3, the product was also nanorods but smaller and longer than those for the pH 2. They were about 30 nm in diameter and up to several micrometers. Most of the nanorods were straight and uniform along their axial axes. For the pH range of 4–10, the products were nanoparticles.

TEM image and SAED patterns of the products were characterized. Figure 4(a) shows a petal of $CeVO_4$ microflowers synthesized at the pH 1 by the microwave radiation. The SAED pattern (Figure 4(b)) shows a number of bright spots of fully concentric rings, which indicated the as-synthesized nanocrystals with different orientations. The rings correspond to the (101), (200), (202), and (321) planes and were specified as tetragonal structured $CeVO_4$. The SAED pattern (Figure 4(c)) confirmed that the petal was single nanocrystals of tetragonal structured $CeVO_4$ with the [–103] direction as zone axis. An electron diffraction pattern with the [–103] zone axis (Figure 4(d)), simulated using CaRIne Crystallography 3.1 [23], corresponds very well with that of Figure 4(c). In addition, the CaRIne Crystallography 3.1 [23] was used to simulate the crystal structure of tetragonal $CeVO_4$ as shown in Figure 5. The sites and fractional coordinates [24] are shown in Table 1. The tetragonal $CeVO_4$ is composed of VO_4 tetrahedral sharing corners and edges with CeO_8 dodecahedral chains. The chains, interrupted by distorted VO_4 units, extended along the c-crystalline axis and were

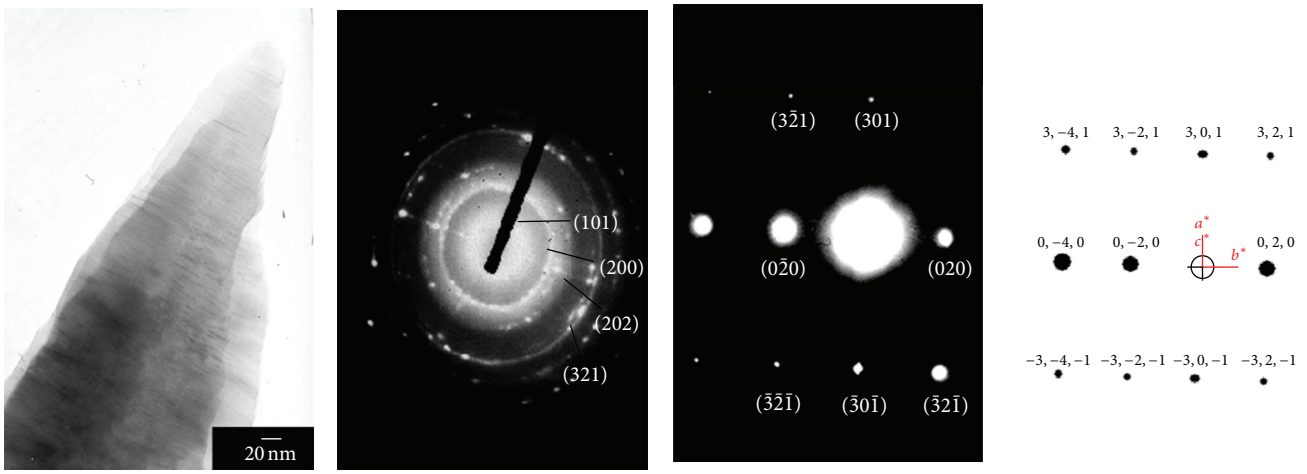

FIGURE 4: (a) TEM image, ((b), (c)) SAED, and (d) simulated patterns of $CeVO_4$ synthesized in the solution with the pH of 1 by microwave radiation at 180 W for 120 min.

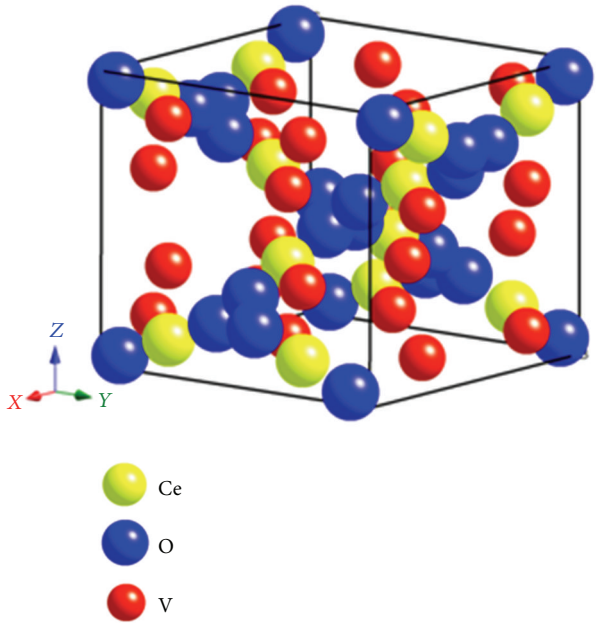

FIGURE 5: Crystal structure of tetragonal $CeVO_4$.

TABLE 1: Lattice sites and fractional coordinates of $CeVO_4$ [24].

Atoms	Sites	x	y	z
Ce	4a	0	0.7500	0.1250
V	4b	0	0.2500	0.3750
O	16h	0	0.4289	0.2053

favorable to stabilizing Ce^{3+} cations even in an oxidizing condition [3, 6, 10].

Due to the above, the as-synthesized $CeVO_4$ was influenced by pH of precursor solutions, with the optimal pH of ≤10. This phenomenon was able to be used for explanation of the complex interaction and balance between the chemical potential and the rate of ionic motion [13]. The morphologies evolution of the products was developed in sequence, nanoparticles → nanorods → microflowers, by decreasing in the pH values of the solutions. Thus possible reactions could be discussed as follows. When cerium source was dissolved in water, $Ce(OH)_3$ formed in alkaline solutions. At high pH values, the formation of VO_4^{3-} was favor, and $CeVO_4$ was synthesized under appropriate heating microwave condition. These led to favor the formation of $CeVO_4$ nanoparticles. In acidic solutions, vanadate species exist as anionic oligomers and Ce^{3+} reactive species as cations. Ce^{3+} existing as mobile cations incorporated with vanadate anions to synthesize $CeVO_4$ [11, 17]:

$$Ce^{3+} + 3OH^- \longrightarrow Ce(OH)_3 \quad (1)$$

$$VO_3^- + OH^- \longrightarrow VO_4^{3-} + H^+ \quad (2)$$

$$Ce(OH)_3 + VO_4^{3-} \longrightarrow CeVO_4 + 3OH^- \quad (3)$$

$$Ce(OH)_3 + 3H^+ \longrightarrow Ce^{3+} + 3H_2O \quad (4)$$

The effect of pH on the morphologies of $CeVO_4$ is presented in Figure 6. It shows the probable growth mechanism of the nanostructures with different morphologies, explaining the structural evolution of $CeVO_4$ under the influence of pH of the precursor solutions. The chemical growth of materials related to the precipitation process of solids from solutions. Basically, they consisted of nucleation and growth stages [25], which balance between the kinetic and thermodynamic growth regimes and strongly control the final nanostructured morphologies [25]. The shapes of the crystals were determined by specific surface energies associated with the crystalline facets [26]. The further development of crystallites was controlled by the hindrance of H^+ on the facets [26]. In this experiment, Ce^{3+} and

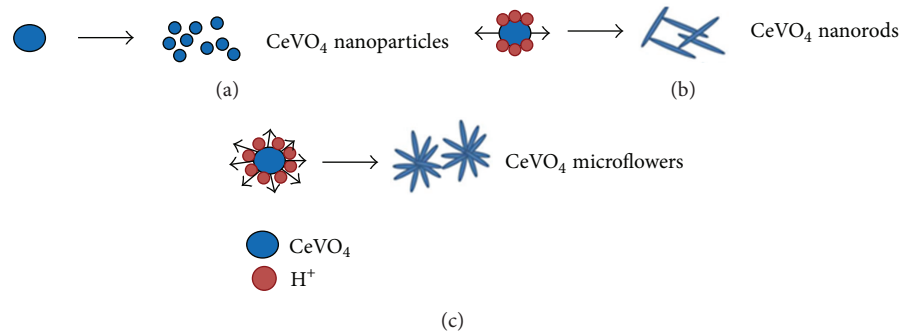

FIGURE 6: Schematic diagram for the formation of $CeVO_4$ microflowers, nanorods, and nanoparticles.

VO_4^{3-} incorporated into crystal lattice of the as-synthesized crystallites which grew according to the anisotropic structure of $CeVO_4$ nanoparticles. Upon decreasing the pH values, the concentrations of H^+ ions were increased. At the pH 3, each facet of the crystallites has the probability to generate active sites by the adsorption of H^+ ions. Then $CeVO_4$ could be grown as 1D nanorods. Until at the pH 1, Ce^{3+} and VO_4^{3-} ions were able to incorporate into the active sites through the more hindrance of adsorbed H^+ ions, leading to the possible formation of microflowers [26].

The UV-visible absorption spectra of the as-synthesized $CeVO_4$ microflowers (pH = 1) and nanorods (pH = 2) are shown in Figure 7. By dispersing of the as-synthesized products in ethanol and sonication of the mixtures for 30 min, the clear solutions formed. The results show strong absorption peaks at 253 and 248 nm for $CeVO_4$ microflowers and nanorods, respectively. A shoulder at 270 nm was also detected for the microflowers. These prominent peaks were attributed to the UV absorption of the VO_4^{3-} of rare earth vanadates [1, 2, 10, 22]. They attributed to the charge transfer from the oxygen ligands to the central vanadium atoms inside the VO_4^{3-} groups of cerium orthovanadate [1, 22]. Obviously, with the decreasing in sizes, the positions of absorption peaks of the as-synthesized $CeVO_4$ products significantly shifted to lower wavelength. It is a typical phenomenon of the quantum-size effect of nanostructured system. $CeVO_4$ has the potential to apply as counter electrodes in electrochromic devices. The blue shift of the absorption peaks affected the electrochromic property of $CeVO_4$-based devices [11]. From UV-visible spectroscopic results, the energy gaps were estimated to be 3.65 and 3.77 eV caused by the optical measurements of $CeVO_4$ microflowers and nanorods, respectively. In addition, optical property of the products was also analyzed by photoluminescence (PL) spectroscopy technique. Figure 8 shows two broad emission bands of $CeVO_4$ microflowers and nanorods centered at 578 and 582 nm, respectively. They could be specified as the electronic transitions from the lowest excited states arising from $5d^1$ to the $4f^1$ ground state ($^2F_{5/2}$ and $^2F_{7/2}$) of the Ce^{3+} ions. The asymmetric emission band was possibly caused by the splitting of the $4f^1$ ground state due to spin-orbital interaction [20].

The band gap values of $CeVO_4$ products obtained by the UV-vis spectroscopy technique are comparable to the band gap value of the well-known photocatalyst [2]. The orthovanadates were reported to act as photocatalysts under UV

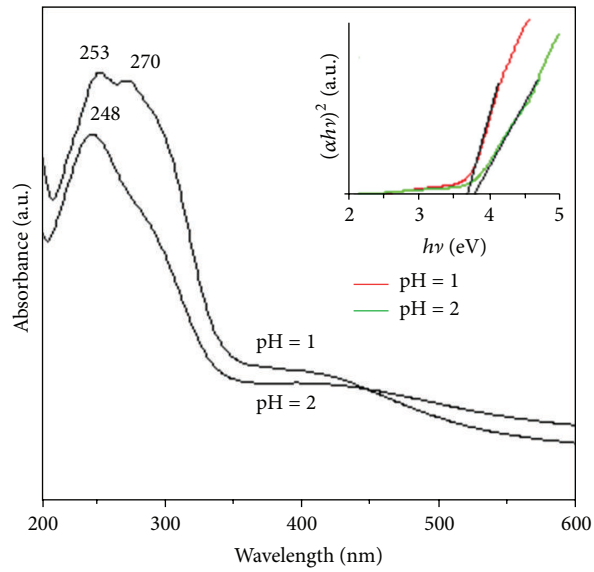

FIGURE 7: (a) UV-visible absorption spectra and (b) the $(\alpha h\nu)^2$ versus $h\nu$ plots of $CeVO_4$ microflowers (pH = 1) and $CeVO_4$ nanorods (pH = 2) synthesized by microwave radiation at 180 W for 120 min.

light [2, 4]. Degradation of MB was used as an indicator to examine the photocatalytic activities of $CeVO_4$ under UV light. The degradation of MB specified from the absorbance spectra of the dye solutions recorded at different time intervals after the recovery of the photocatalyst. The highest intensities of the UV-visible spectra of MB at 665 nm wavelength for $CeVO_4$ synthesized in the solutions with the pH of 1 (microflowers) and 2 (nanorods) under UV light were monotonically decreased within 35 min. The reaction mechanism for the degradation of MB by pure $CeVO_4$ was discussed according to the following. When the solutions were irradiated by UV light, MB molecules were excited. Subsequently, the photoexcited electrons transferred to conduction band of $CeVO_4$ and further transferred to the adsorbed O_2 on the surface of $CeVO_4$ to form $\bullet O_2$ negative superoxide radicals. At the same time, protonation of OH^- or H_2O yielded $\bullet OH$ radicals, which were responsible for the degradation of MB molecules [27, 28].

Figure 9 shows the MB degradation efficiency of $CeVO_4$ nanostructure under UV light within different lengths of

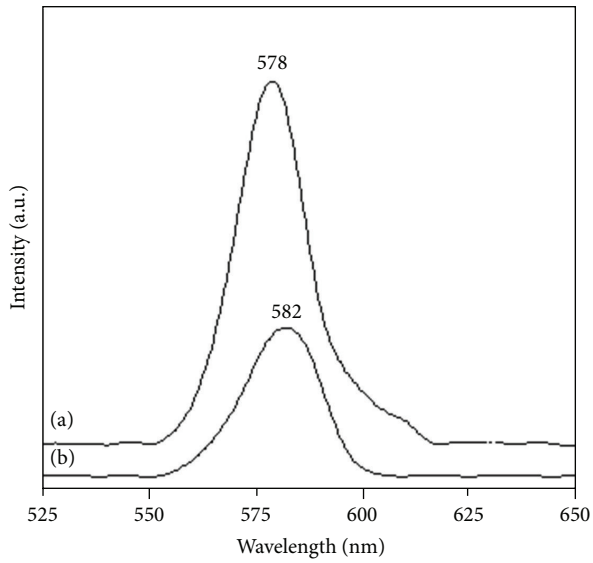

FIGURE 8: PL spectra of (a) $CeVO_4$ microflowers (pH = 1) and (b) $CeVO_4$ nanorods (pH = 2) synthesized by microwave radiation at 180 W for 120 min.

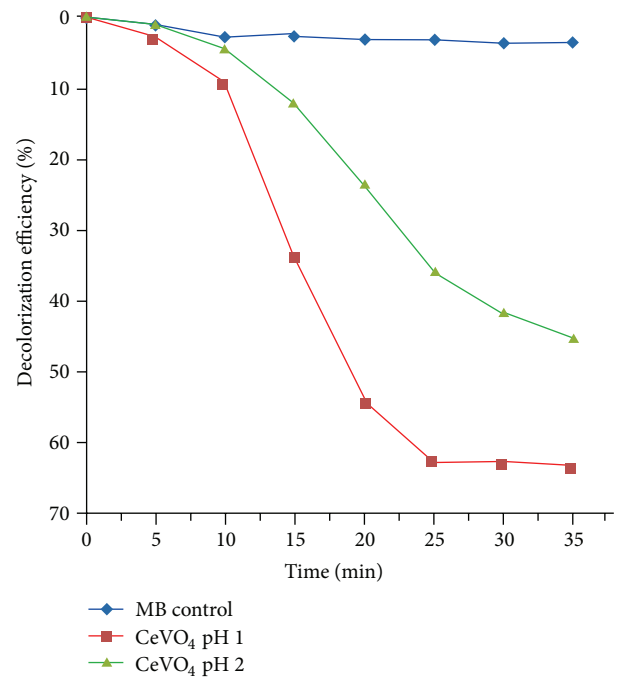

FIGURE 9: Photodegradation of methylene blue under UV light by $CeVO_4$ synthesized in the solutions with the pH of 1 and 2, compared to the MB control (catalyst-free solution).

time, compared to the control or catalyst-free solution. Concentration of MB rapidly decreased to 63% and 45% for the as-synthesized $CeVO_4$ microflowers and nanorods, respectively. These show that $CeVO_4$ microflowers have 18% higher photocatalytic activity than $CeVO_4$ nanorods. The space between internanorods of $CeVO_4$ microflowers could function effectively in promoting reflection of trapped incident light, enhance light harvesting, and increase the quantities of photogenerated electrons and holes participating in the photocatalysis [29, 30]. Size and crystalline nature of the photocatalyst played a critical role in determining the photocatalytic activity of the present study. Shape of the crystals influenced the absorbance and direct energy gap, which reflected the photocatalytic performance due to the different activities of the dominant facets [31–33]. In this research, the energy gap of $CeVO_4$ microflowers synthesized at the pH of 1 is narrower than the energy gap of $CeVO_4$ nanorods synthesized at the pH of 2. The specific surface, controlled by structure and crystallite size, was an important factor to determine the reaction activity. The higher photocatalytic activity of $CeVO_4$ microflowers could pertain to defects containing in grain boundaries, surficial amorphous layers, and intergranular layers [34]. The present analysis is able to contribute to the potential application of $CeVO_4$ microflowers for waste water treatment.

4. Conclusions

In this paper, we have developed a microwave radiation method for synthesizing nanostructured cerium orthovanadate. This system is simple and efficient in controlling different morphologies of the products. The pH of the precursor solutions was the key factor to control the morphologies of $CeVO_4$: nanoparticles, nanorods, and microflowers. In this research, the growth mechanism was proposed the role of pH of the precursor solutions in synthesizing $CeVO_4$ nanostructures. Energy gaps of the as-synthesized $CeVO_4$ were 3.65 eV for microflowers and 3.77 eV for nanorods. The photocatalytic activity of these materials was identified by the degradation of MB. The activity of $CeVO_4$ microflowers was higher than that of $CeVO_4$ nanorods.

Acknowledgments

The authors wish to thank the Thailand Office of the Higher Education Commission for providing financial support through the National Research University (NRU) Project for Chiang Mai University and the Human Resource Development Project in Science Achievement Scholarship of Thailand (SAST). They also acknowledge the National Nanotechnology Center (NANOTEC), National Science and Technology Development Agency, for providing financial support through the project P-10-11345, and the Graduate School of Chiang Mai University through a general support.

References

[1] J. Liu and Y. Li, "General synthesis of colloidal rare earth orthovanadate nanocrystals," *Journal of Materials Chemistry*, vol. 17, no. 18, pp. 1797–1803, 2007.

[2] R. K. Selvan, A. Gedanken, P. Anilkumar, G. Manikandan, and C. Karunakaran, "Synthesis and characterization of rare earth orthovanadate (RVO4; R = La, Ce, Nd, Sm, Eu & Gd) nanorods/nanocrystals/nanospindles by a facile sonochemical method and their catalytic properties," *Journal of Cluster Science*, vol. 20, no. 2, pp. 291–305, 2009.

[3] F. Luo, C.-J. Jia, W. Song, L.-P. You, and C.-H. Yan, "Chelating ligand-mediated crystal growth of cerium orthovanadate," *Crystal Growth and Design*, vol. 5, no. 1, pp. 137–142, 2005.

[4] S. Mahapatra, G. Madras, and T. N. G. Row, "Synthesis, characterization and photocatalytic activity of lanthanide (Ce, Pr and Nd) orthovanadates," *Industrial and Engineering Chemistry Research*, vol. 46, no. 4, pp. 1013–1017, 2007.

[5] U. Opara Krašovec, B. Orel, A. Šurca, N. Bukovec, and R. Reisfeld, "Structural and spectroelectrochemical investigations of tetragonal $CeVO_4$ and Ce/V-oxide sol-gel derived ion-storage films," *Solid State Ionics*, vol. 118, no. 3-4, pp. 195–214, 1999.

[6] R. Jindal, M. M. Sinha, and H. C. Gupta, "Lattice vibrations of AVO_4 crystals (A = Lu, Yb, Dy, Tb, Ce)," *Spectrochimica Acta Part A*, vol. 113, pp. 286–290, 2013.

[7] F. Liu, X. Shao, Y. Yin et al., "Selective synthesis and growth mechanism of $CeVO_4$ nanoparticals via hydrothermal method," *Journal of Rare Earths*, vol. 29, no. 2, pp. 97–100, 2011.

[8] A. B. Garg, K. V. Shanavas, B. N. Wani, and S. M. Sharma, "Phase transition and possible metallization in $CeVO_4$ under pressure," *Journal of Solid State Chemistry*, vol. 203, pp. 273–280, 2013.

[9] S. Mahapatra, S. K. Nayak, G. Madras, and T. N. Guru Row, "Microwave synthesis and photocatalytic activity of nano lanthanide (Ce, Pr, and Nd) orthovanadates," *Industrial and Engineering Chemistry Research*, vol. 47, no. 17, pp. 6509–6516, 2008.

[10] L. Zhu, Q. Li, J. Li, X. Liu, J. Meng, and X. Cao, "Selective synthesis of mesoporous and nanorod $CeVO_4$ without template," *Journal of Nanoparticle Research*, vol. 9, no. 2, pp. 261–268, 2007.

[11] H. Wang, Y. Meng, and H. Yan, "Rapid synthesis of nanocrystalline $CeVO_4$ by microwave irradiation," *Inorganic Chemistry Communications*, vol. 7, no. 4, pp. 553–555, 2004.

[12] J. L. F. Da Silva, M. V. Ganduglia-Pirovano, and J. Sauer, "Formation of the cerium orthovanadate $CeVO_4$: DFT+U study," *Physical Review B*, vol. 76, Article ID 125117, 2007.

[13] L. Chen, "Hydrothermal synthesis and ethanol sensing properties of $CeVO_4$ and $CeVO_4$-CeO_2 powders," *Materials Letters*, vol. 60, no. 15, pp. 1859–1862, 2006.

[14] Y. Chen, C. Lu, L. Xu, Y. Ma, W. Hou, and J.-J. Zhu, "Single-crystalline orthorhombic molybdenum oxide nanobelts: synthesis and photocatalytic properties," *CrystEngComm*, vol. 12, no. 11, pp. 3740–3747, 2010.

[15] Y. Yan, X. Liu, W. Fan, P. Lv, and W. Shi, "InVO4 microspheres: preparation, characterization and visible-light-driven photocatalytic activities," *Chemical Engineering Journal*, vol. 200–202, pp. 310–316, 2012.

[16] P. Madhusudan, J. Ran, J. Zhang, J. Yu, and G. Liu, "Novel urea assisted hydrothermal synthesis of hierarchical $BiVO_4$/$Bi_2O_2CO_3$ nanocomposites with enhanced visible-light photocatalytic activity," *Applied Catalysis B*, vol. 110, pp. 286–295, 2011.

[17] B. Xie, G. Lu, Q. Dai, Y. Wang, Y. Guo, and Y. Guo, "Synthesis of $CeVO_4$ crystals with different sizes and shapes," *Journal of Cluster Science*, vol. 22, no. 4, pp. 555–561, 2011.

[18] A. B. Panda, G. Glaspell, and M. Samy El-Shall, "Microwave synthesis and optical properties of uniform nanorods and nanoplates of rare earth oxides," *Journal of Physical Chemistry C*, vol. 111, no. 5, pp. 1861–1864, 2007.

[19] Powder Diffraction File, JCPDS-ICDD, Newtown Square, Pa, USA, 19073–3273, 2001.

[20] H. Deng, S. Yang, S. Xiao, H.-M. Gong, and Q.-Q. Wang, "Controlled synthesis and upconverted avalanche luminescence of cerium(III) and neodymium(III) orthovanadate nanocrystals with high uniformity of size and shape," *Journal of the American Chemical Society*, vol. 130, no. 6, pp. 2032–2040, 2008.

[21] B. Orel, A. Šurca Vuk, U. Opara Krašovec, and G. Dražič, "Electrochromic and structural investigation of $InVO_4$ and some other vanadia-based oxide films," *Electrochimica Acta*, vol. 46, no. 13-14, pp. 2059–2068, 2001.

[22] T.-D. Nguyen, C.-T. Dinh, and T.-O. Do, "Monodisperse samarium and cerium orthovanadate nanocrystals and metal oxidation states on the nanocrystal surface," *Langmuir*, vol. 25, no. 18, pp. 11142–11148, 2009.

[23] C. Boudias and D. Monceau, CaRIne Crystallography 3.1, DIVERGENT S.A., Centre de Transfert, 60200 Compiègne, France, 1989–1998.

[24] V. Panchal, S. López-Moreno, D. Santamaría-Pérez et al., "Zircon to monazite phase transition in $CeVO_4$: X-ray diffraction and Raman-scattering measurements," *Physical Review B*, vol. 84, Article ID 024111, 2011.

[25] G. Liu, X. Duan, H. Li, and H. Dong, "Hydrothermal synthesis, characterization and optical properties of novel fishbone-like $LaVO_4$:Eu^{3+} nanocrystals," *Materials Chemistry and Physics*, vol. 115, no. 1, pp. 165–171, 2009.

[26] X. Wang, H. Xu, H. Wang, and H. Yan, "Morphology-controlled $BaWO_4$ powders via a template-free precipitation technique," *Journal of Crystal Growth*, vol. 284, no. 1-2, pp. 254–261, 2005.

[27] J. Yu, G. Dai, Q. Xiang, and M. Jaroniec, "Fabrication and enhanced visible-light photocatalytic activity of carbon self-doped TiO_2 sheets with exposed 001 facets," *Journal of Materials Chemistry*, vol. 21, no. 4, pp. 1049–1057, 2011.

[28] Q. Xiang, J. Yu, and P. K. Wong, "Quantitative characterization of hydroxyl radicals produced by various photocatalysts," *Journal of Colloid and Interface Science*, vol. 357, no. 1, pp. 163–167, 2011.

[29] Q. Xiang, B. Cheng, and J. Yu, "Hierarchical porous CdS nanosheet-assembled flowers with enhanced visible-light photocatalytic H2-production performance," *Applied Catalysis B*, vol. 138-139, pp. 299–303, 2013.

[30] X. Yu, J. Yu, B. Cheng, and M. Jaroniec, "Synthesis of hierarchical flower-like AlOOH and TiO_2/AlOOH superstructures and their enhanced photocatalytic properties," *Journal of Physical Chemistry C*, vol. 113, no. 40, pp. 17527–17535, 2009.

[31] B. Cheng, W. Wang, L. Shi, J. Zhang, J. Ran, and H. Yu, "One-pot template-free hydrothermal synthesis of monoclinic $BiVO_4$ hollow microspheres and their enhanced visible-light photocatalytic activity," *International Journal of Photoenergy*, vol. 2012, Article ID 797968, 10 pages, 2012.

[32] M. Umadevi and A. J. Christy, "Synthesis, characterization and photocatalytic activity of CuO nanoflowers," *Spectrochimica Acta Part A*, vol. 109, pp. 133–137, 2013.

[33] Y. Fang, Z. Li, S. Xu, D. Han, and D. Lu, "Optical properties and photocatalytic activities of spherical ZnO and flower-like ZnO structures synthesized by facile hydrothermal method," *Journal of Alloys and Compounds*, vol. 575, pp. 359–363, 2013.

[34] L. Qi, H. Li, and L. Dong, "Simple synthesis of flower-like ZnO by a dextran assisted solution route and their photocatalytic degradation property," *Materials Letters*, vol. 107, pp. 354–356, 2013.

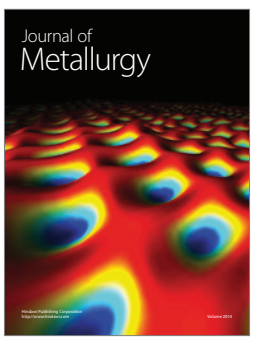

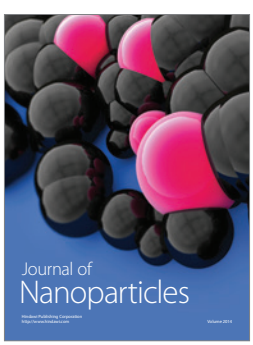

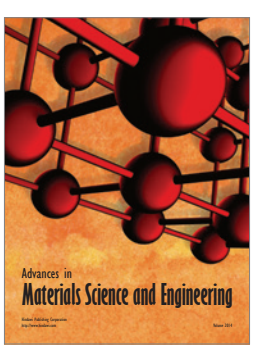

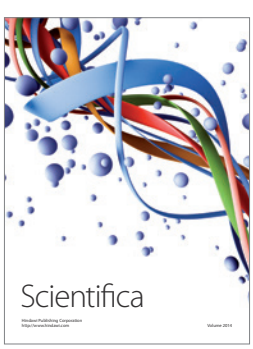

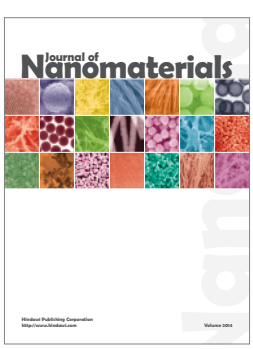

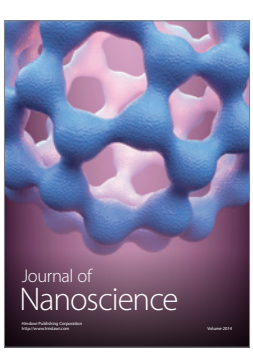

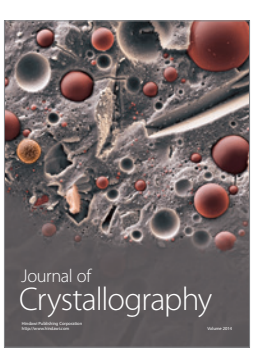

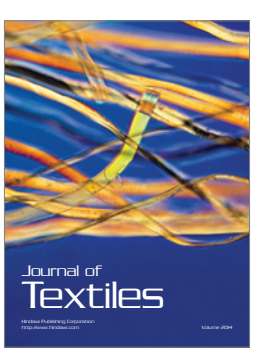

Hindawi

Submit your manuscripts at
http://www.hindawi.com